The influence of energetic bombardment on the structure and properties of epitaxial $SrRuO_3$ thin films grown by pulsed laser deposition

J-P. Maria, S. Trolier-McKinstry, and D. G. SchlomM. E. Hawley and G. W. Brown

Citation: **83**, (1998); doi: 10.1063/1.367195
View online: http://dx.doi.org/10.1063/1.367195
View Table of Contents: http://aip.scitation.org/toc/jap/83/8
Published by the American Institute of Physics

The influence of energetic bombardment on the structure and properties of epitaxial $SrRuO_3$ thin films grown by pulsed laser deposition

J-P. Maria,[a] S. Trolier-McKinstry, and D. G. Schlom
Department of Materials Science and Engineering, Intercollege Materials Research Laboratory, The Pennsylvania State University, University Park, Pennsylvania 16802

M. E. Hawley and G. W. Brown
Center for Materials Science, Los Alamos National Laboratory, Los Alamos, New Mexico 87545

(Received 10 November 1997; accepted for publication 21 January 1998)

$SrRuO_3$ epitaxial thin films were prepared by pulsed laser deposition (PLD) under a range of growth conditions to study the impact of bombardment on properties. Growth conditions favoring energetic bombardment resulted in $SrRuO_3$ films with expanded in-plane and out-of-plane lattice constants. In particular, $SrRuO_3$ films with pseudocubic out-of-plane lattice constants as large as 4.08 Å were deposited (3.8% larger than the bulk value). Those films with expanded lattices had greater resistivities and depressed Curie transition temperatures. The relative lattice mismatch between film and substrate was found to temper the effect of bombardment such that as the mismatch increased, a higher degree of bombardment was required to produce extended lattice parameters. The pressure-dependent energetic species inherent to PLD and their interaction with the ambient are believed to be the source of the bombarding flux. Further experiments confirmed that in the range of 20–200 mTorr, oxygen/ozone partial pressure had a negligible effect on the film properties. © *1998 American Institute of Physics.* [S0021-8979(98)09408-0]

I. INTRODUCTION

The low resistivity of $SrRuO_3$ (275 $\mu\Omega$ cm at room temperature) coupled with the 3.93 Å lattice spacing of its perovskite cell make it an attractive material for electrodes in heterostructures incorporating a variety of perovskite-based ferroelectric, dielectric, and superconducting films.[1] At room temperature, $SrRuO_3$ exhibits the $GdFeO_3$ orthorhombic structure, space group *Pnma*, but may be indexed as a pseudocubic perovskite with a RuO_6 octahedral tilt of $\sim 0.1°$.[2–4] $SrRuO_3$ undergoes a ferromagnetic transition at 160 K as evidenced by discontinuities in both the magnetic susceptibility and resistivity temperature profiles.[1] Since $SrRuO_3$, and the closely related Ruddlesden–Popper phase, $Sr_3Ru_2O_7$, have been the only known ferromagnetic perovskite crystals resulting from a second row $4d$ transition metal, much interest has been generated among researchers in this material.[5–7] In addition, the remarkable chemical and thermal stability of $SrRuO_3$ make it a candidate for microelectromechanical systems (MEMS), specifically those designed to transport aggressive fluids.

As the quality of many electronic heterostructures or MEMS will ultimately rely upon the structural and electrical properties of the underlying electrodes, an understanding of the processing property relationships in $SrRuO_3$ epitaxial films is required. Results are presented which illustrate the strong structure-property dependence of $SrRuO_3$ films on pulsed laser deposition (PLD) processing conditions. Specifically, the importance of energetic bombardment, oxygen pressure, and substrate/film lattice mismatch are described.

[a]Electronic mail: jpm133@psu.edu

II. EXPERIMENTAL PROCEDURE

Epitaxial $SrRuO_3$ thin films were pulsed laser deposited on vicinal (001) $SrTiO_3$ and nominal (001) $LaAlO_3$ (perovskite subcell indices) substrates supplied by Commercial Crystal Laboratories and Lucent Technologies, respectively. All substrates were cleaned prior to deposition by a 5 min sonication in each of the following fluids in the order: micro cleaning solution,[8] deionized water, acetone, ethanol, and isopropanol. To provide a smooth and TiO_2-terminated surface, the $SrTiO_3$ substrates were further treated by etching in buffered HF solution.[9] The substrates were fixed to a conductive block heater with silver paint. The deposition temperature for all films was 680 °C (as measured by a *K*-type thermocouple embedded in the heater block center). A target-to-substrate distance of 8 cm was used for all depositions. An atmosphere of 10% ozone, balance molecular oxygen (i.e., the output of PCI-1 ozone generator[10]) in the pressure range of 20–160 mTorr was maintained; argon was introduced when desired. The chamber pressure was measured with a Baratron[11] capacitance manometer due to its insensitivity to gas composition. To ablate material, a Lambda Physik EMG 150 KrF excimer laser operating at 248 nm, $\sim$200 mJ pulses, and a frequency of 10 Hz, was focused to an energy density of ~ 2 J/cm^2 upon a stoichiometric, rotating, hot-pressed ceramic target.[12]

Structural characterization was performed using a Picker four-circle x-ray diffractometer (XRD) equipped with a graphite monochromator. From measurement of the 400 reflection of single crystal silicon, instrumental resolutions of 0.15° and 0.25° in 2θ and ω, respectively, were determined. Resolution in the ϕ-circle was 0.4°, as measured from the 220 reflection of the same Si crystal. The Nelson–Riley

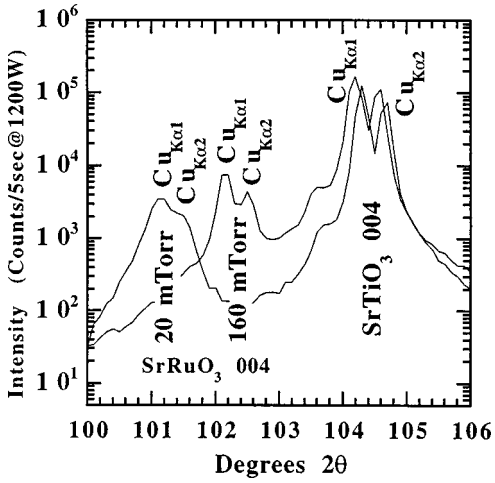

FIG. 1. θ-2θ x-ray diffraction pattern showing the $SrRuO_3$ 004_{perov} (440_{ortho}) reflection for films grown at 20 and 160 mTorr. The FWHM of both film peaks is 0.25° in 2θ.

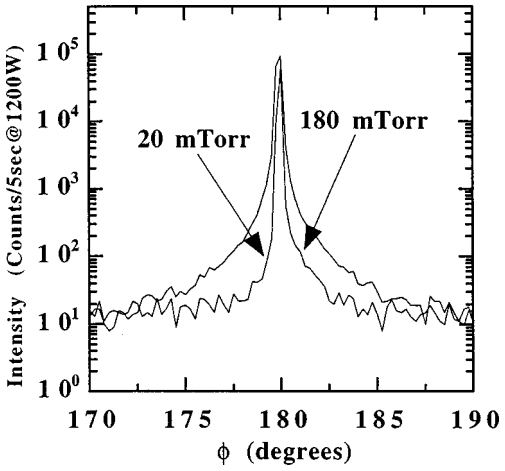

FIG. 2. The ϕ-scan of the $SrRuO_3$ 101_{perov} (112_{ortho}) reflection for films grown at 20 and 160 mTorr. The FWHMs of the peaks in ϕ are 0.35° and 0.30°, respectively.

method (which uses a family of reflections, thus accounting for height adjustment errors and absorption effects) was used to calculate out-of-plane d-spacings.[13]

The temperature dependence of the resistivity was determined by four-point probe resistance measurements on the $SrRuO_3$ films while they were slowly immersed into a liquid helium dewar. Current was applied to the outer electrodes with a Keithley 220 current source, while the voltage drop across the inner electrodes was measured with a HP 34401A multimeter. Contacts to the dc diode sputtered gold electrodes were made by aluminum wire bonding. Resistivity measurements were made within a few hours of wire bonding; thus, no influence on the measurement is expected from the formation of Au–Al intermetallic phases.[14] Profilometry[15] was used to determine the thicknesses of the $SrRuO_3$ layers by scanning over a shadowmasked film edge. Finally, the surface morphology was imaged with a Nanoscope III STM. Surface images were collected in constant current mode with a sample bias of 1.2 V and a current setpoint of 70 pA. Both etched and machined PtIr tips were employed. Multiple scans of each film were collected to ensure that those presented are representative of the film's surface structure.

III. RESULTS AND DISCUSSION

A. Structural analysis

Initially, $SrRuO_3$ films were deposited on the etched $SrTiO_3$ substrates at deposition pressures of 20 and 160 mTorr O_3/O_2; all other processing conditions identical. The structural analysis as determined by four-circle XRD is shown in Figs. 1, 2, and 3, along with the calculated pseudocubic lattice parameters. Epitaxial growth is confirmed over all angles examined. Expanded sections are shown to make the differences between the patterns easily discernable. In the θ-2θ pattern (Fig. 1) it is clear that in comparison to bulk values, the out-of-plane lattice constants in both films are expanded. Out-of-plane pseudocubic lattice constants for the 160 and 20 mTorr samples are 3.95 and 4.04 Å (± 0.01 Å). From measurement of the 103_{perov} reflection, the in-plane constants of both films were determined to be 3.95 ± 0.02 Å. Full width at half maximum (FWHM) values in all circles were nearly identical in both films, indicating that the majority of the material in both cases was of similar crystalline perfection. However, when the full width at quarter maximum values are compared, it becomes clear that the linewidths are much greater for the heavily bombarded sample, i.e., the one grown at pressures where the incident species are not thermalized prior to striking the substrate.[16] This feature is indicative of a smaller fraction of the crystal which is more disordered or distorted with respect to the substrate and its orientation.

Between PLD depositions at 20 and 160 mTorr O_3/O_2 two major differences exist: (i) the concentration of oxidant and (ii) the energy and flux of bombarding species impinging upon the growing film. In an attempt to determine which factor had the greatest influence, a third set of processing conditions using the off-axis geometry[17] (i.e., the substrate and target normals are orthogonal) were employed. Figure 4

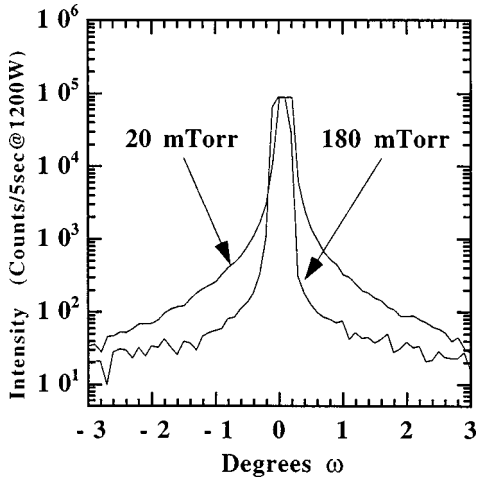

FIG. 3. Rocking curve of the $SrRuO_3$ 002_{perov} (220_{ortho}) reflection for films grown at 20 and 160 mTorr. The FWHM of both peaks in ω is 0.26°.

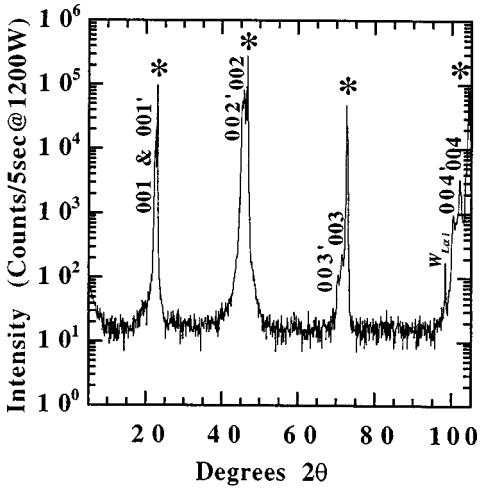

FIG. 4. θ-2θ x-ray diffraction scan of a $SrRuO_3$ film grown by 90° off-axis PLD. The peaks in this and other off-axis scans indicate the presence of two epitaxial phases; one with lattice constants close to the bulk $SrRuO_3$ phase ($a_0 = 3.95 \pm 0.02$ Å) and another with swelled lattice constants ($a = 4.01 \pm 0.02$ Å, $c = 4.02 \pm 0.01$ Å). The x-ray reflections from the swelled phase are indexed as hkl'. The substrate peaks are marked by asterisks (*), and the peaks marked with $WL_{\alpha l}$ are due to x-rays with $WL_{\alpha l}$ wavelength diffracting off the nearby substrate peaks.

shows a θ-2θ diffraction pattern for an off-axis deposited film in the presence of 20 mTorr O_3/O_2. A second set of peaks [indicated by the prime mark ($'$) in Fig. 4] were found and appear to be due to an additional epitaxial phase (epitaxy of this phase was confirmed by in-plane x-ray scans). The two $SrRuO_3$ phases have pseudocubic unit cells with lattice constants of 3.95 and 4.02 Å. Indeed these deposition conditions resulted in the film showing features of both the high and low pressure on-axis deposited material. Ideally, the off-axis geometry would offer bombardment-free deposition, but the possibilities of large compositional and microstructural differences between on and off-axis films prohibits reliable comparison to on-axis growth conditions.[18]

To study the importance of oxygen content in the ambient gas, $SrRuO_3$ films were deposited under a fourth set of deposition conditions. These conditions were identical to those of the high pressure deposited films with the exception that the atmosphere was composed of 20 mTorr O_3/O_2 and 140 mTorr Ar. In this hybrid atmosphere the oxidizing ability should be similar to that of 20 mTorr O_3/O_2, yet, due to the similarities in the scattering cross sections of Ar and O_2, the bombardment experienced by the film during deposition should be similar to that during deposition under 160 mTorr O_3/O_2.[19] X-ray analysis on this film confirmed a pseudocubic structure with a lattice constant of 3.94 ± 0.01 Å; identical to within the resolution of our diffractometer to the high pressure deposited $SrRuO_3$. This experiment indicates that within the pressure range of 20–160 mTorr, $SrRuO_3$ shows no structural dependence on oxygen partial pressure, thus the differences between the 20 and 160 mTorr deposited films are most likely a result of energetic bombardment during growth.

$SrRuO_3$ films were also deposited on $LaAlO_3$ substrates. Again, as shown in Table I, under high bombardment growth conditions, expanded lattice constants are observed. However, for films deposited on $LaAlO_3$, to achieve similarly extended lattice constants, more intense bombardment was necessary and was provided by further reducing the deposition pressure or decreasing the target-to-substrate separation distance. This suggests that as the lattice mismatch between the $SrRuO_3$ films and the substrates becomes larger, to observe similarly extended lattice parameters, a greater energetic species flux or larger species energy is required. Table I lists the substrates, deposition parameters, and lattice constants of the $SrRuO_3$ thin films.

TABLE I. Processing conditions and lattice constants for $SrRuO_3$ films deposited on $SrTiO_3$ and $LaAlO_3$ substrates.

Substrate	Processing conditions	Lattice constants (Å)
$SrTiO_3$ (001)	160 mTorr O_3/O_2	$a = c = 3.95$
$SrTiO_3$ (001)	20 mTorr O_3/O_2	$a = 3.95$, $c = 4.04$
$SrTiO_3$ (001)	20 mTorr O_3/O_{2+} 140 mTorr Ar	$a = c = 3.95$
$SrTiO_3$ (001)	20 mTorr O_3/O_2 (Off-axis)	$a = c = 3.95$: $a' = c' = 4.01$
$LaAlO_3$ (001)	160 mTorr O_3/O_2	$a = c = 3.93$
$LaAlO_3$ (001)	20 mTorr O_3/O_2	$a = 3.97$, $c = 3.94$

X-ray analysis was performed on the films deposited on $SrTiO_3$ in order to determine the orientation of the orthorhombic cell. Two planes of orthorhombic $SrRuO_3$ are favorable for epitaxial growth on (001) oriented $SrTiO_3$: $(001)_{SRO} \| (001)_{STO}$ and $(110)_{SRO} \| (001)_{STO}$. As reported previously, the location of off-axis $SrRuO_3$ 113 x-ray reflections allows determination of the orientation.[3] Figure 5 shows this data for a 160 mTorr deposited $SrRuO_3$ film. The χ-angle at which the 113 reflections were observed indicates that the film is oriented with $(110)_{SRO} \| (001)_{STO}$; no material oriented with $(001)_{SRO} \| (001)_{STO}$ was detected. The twofold symmetry indicates that the ruthenate film is single domain, and oriented with its c axis in the plane of the substrate parallel to the [100] $SrTiO_3$ direction, but not parallel to the [010] $SrTiO_3$ direction. The vicinal $SrTiO_3$ (001) surface (misoriented by $0.5° \pm 0.2°$ toward [010] and $0.0° \pm 0.2°$ toward

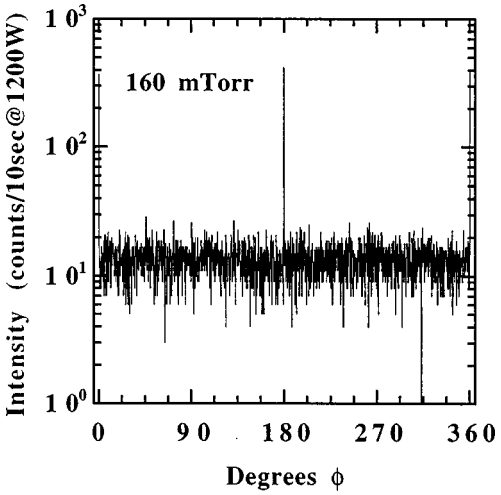

FIG. 5. The ϕ-scan of the $SrRuO_3$ 113_{ortho} peak for a film grown at 160 mTorr on a $SrTiO_3$ (001) substrate misoriented by 0.5° toward $SrTiO_3$ [010]. $\phi = 0°$ is set parallel to the $SrTiO_3$ [100] in-plane direction.

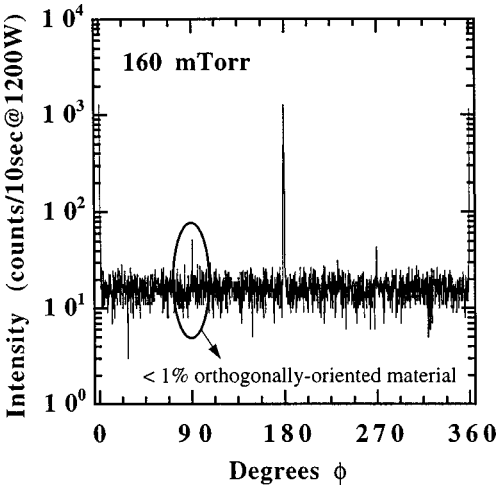

FIG. 6. The ϕ-scan of the $SrRuO_3$ 221_{ortho} peak for a film grown at 160 mTorr on a $SrTiO_3$ (001) substrate misoriented by 0.5° toward $SrTiO_3$ [010]. $\phi = 0°$ is set parallel to the $SrTiO_3$ [100] in-plane direction.

[100]) is sufficient to destroy the fourfold symmetry of the (001) $SrTiO_3$ surface and lead to the growth of untwinned $SrRuO_3$. This is in agreement with previous reports of untwinned $SrRuO_3$ growth on vicinal $SrTiO_3$.[3,20] Having established the $[110]_{SRO}\|[001]_{STO}$ orientation, it is possible to more sensitively detect twinning in the substrate plane by performing a ϕ scan of the more intense 221 $SrRuO_3$ reflection. Figure 6 shows this data. Again, the nearly perfect twofold symmetry is indicative of one predominant in-plane orientation of $SrRuO_3$. Small peaks located at 90° and 270° are a result of orthogonally oriented domains, which from relative peak height intensity calculations account for less than 1 vol % of material. Interestingly, for the 20 mTorr O_3/O_2 film with extended lattice constants, despite its identical substrate misorientation and extensive x-ray examination, neither 113- or 221-type reflections could be observed. Given the large differences in the lattice constants of the heavily bombarded sample, it is possible that the crystal symmetry changed with respect to the bulk material (i.e., destruction of the orthorhombic distortion), resulting in the extinction of these reflections.

It has been previously reported by Gan *et al.*[20] that the ability to grow untwinned $SrRuO_3$ depends strongly upon the cut of the untwinned (001) $SrTiO_3$ substrate: large miscut angles directed along ⟨100⟩ $SrTiO_3$ favored single crystal growth and smaller miscut angles or substrates miscut along ⟨110⟩ directions favored 90° rotation twin formation. The substrates used in this work were miscut by $0.5° \pm 0.02°$ along [100], yet still yielded nearly single crystal films (i.e., less than 1% rotation twins). Larger substrate misorientations were found necessary in the work of Gan *et al.* to suppress twinning.[20] Our result may be due to a longer surface diffusion length for the condensate under PLD growth conditions, or to a reduced substrate step roughness resulting from etching of the substrate prior to growth.

B. Surface analysis

The surface morphology of both films was examined by scanning tunneling microscopy (STM). Figures 7(a) and 7(b)

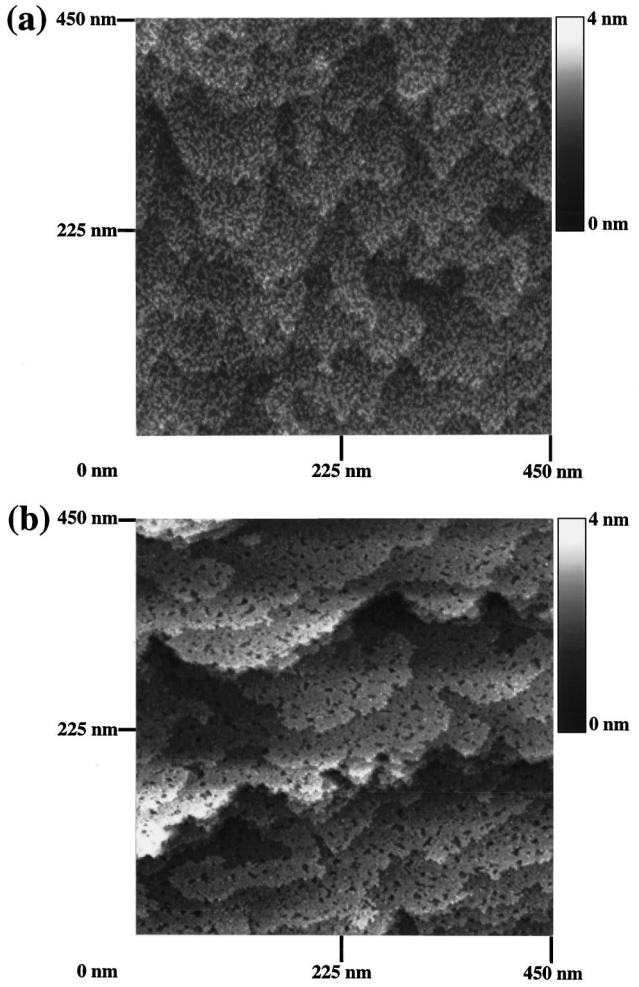

FIG. 7. STM images of the surface of $SrRuO_3$ films grown at (a) 160 mTorr and (b) 20 mTorr. The edges of the images are nearly parallel to ⟨100⟩ $SrTiO_3$. Both images use the same vertical scale.

are surface images of the 160 mTorr O_3/O_2 and 20 mTorr O_3/O_2 deposited $SrRuO_3$. Root mean square surface roughness values of 4.7 and 7.5 Å were determined for the high and low pressure deposited $SrRuO_3$. Both images show terrace structures perpendicular to the direction of miscut which suggests that the films grow by a step-flow mechanism.

Faceting along ⟨110⟩ perovskite directions is observed in the film grown at high pressure. Applying the line intercept method to the STM images, average terrace lengths for the high and low pressure deposited films were calculated to be 55 and 160 nm, respectively. Given the measured miscut angles of the substrates, and assuming single unit cell steps on the etched $SrTiO_3$ surface (which has been confirmed by previous researchers[9]) terrace lengths of 45 nm would be expected. This, together with the absence of a measurable tilt between the substrate and film basal planes indicates that films deposited at higher pressures better maintain the topography of the substrate. The more intense bombardment experienced by the low pressure deposited samples may enhance three-dimensional diffusion during growth and result in films with a coarsened appearance, i.e., supersteps and longer terraces. STM measurements indicated that the average step

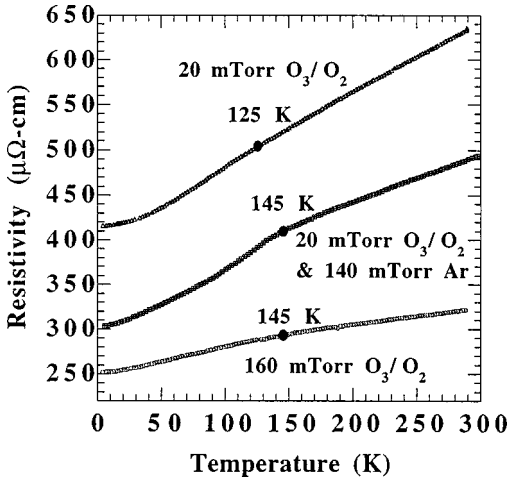

FIG. 8. Resistivity vs temperature curves for $SrRuO_3$ films deposited using three different deposition conditions. Approximate Curie temperatures indicated by black circles.

height is larger on the films deposited under strong bombardment conditions.

Tarsa *et al.*[21] reported similar results for homoepitaxial $SrTiO_3$ thin films. In that work, extended out-of-plane lattice constants were observed when PLD ambient pressures were reduced below 100 mTorr. Though the growth mechanism was not step-flow, roughening of the $SrTiO_3$ film was also observed at lower deposition pressures, all other parameters remaining identical. Since the film growth rate in PLD depends strongly on ambient pressure in the range of 1–300 mTorr,[22] a direct correlation between roughness and bombardment cannot be made, as film growth rate will also influence the final surface morphology.

C. Electrical property measurements

The temperature dependence of the resistance was measured for the $SrRuO_3$ films on $SrTiO_3$ and is shown in Fig. 8. Resistance was measured from 4.2 K to room temperature for the high and low pressure deposited samples as well as the sample prepared in the $Ar/O_3/O_2$ atmosphere. The high pressure O_3/O_2 sample exhibited the lowest resistivity at all temperatures, the low pressure sample the highest. This observation may be explained by assuming that the extended lattice constants incurred from the energetic bombardment result in reduction of the O $2p-$Ru $4d$ orbital overlap, causing an increase in resistivity.[23] A second possibility is that an Anderson-type localization of conduction orbitals occurred as a result of bombardment-induced structural defects or distortions.[23] The Anderson localization mechanism would predict a Mott transition which has been observed by previous researchers on other damaged metallic perovskite films.[24,25] Both the high pressure deposited sample and the $Ar/O_3/O_2$ deposited samples showed Curie transitions occurring at $\sim$145 K, however, the sample deposited in the presence of argon had a larger resistivity and resistivity ratio; the reason for this is not understood. The Curie temperature of the low pressure film occurred at $\sim$120 K; similar depressions of the Curie transition temperature below 160 K have been observed by other researchers.[24,26–28]

The Curie temperature (T_c) of $SrRuO_3$ is known to depend upon hydrostatic pressure; Shikano *et al.*[29] and Neumeier *et al.*[30] reported pressure coefficients of resistivity of -7.9 K/GPa and -5.7 K/GPa, respectively. Though some of the shift in T_c of our films, and those of others, may be due to this pressure effect, the stress state of the $SrRuO_3$ due to thermal expansion mismatch will be biaxial rather than hydrostatic; a loading condition for which the dependence of T_c is unknown. Even if the pressure dependence for biaxial stress is similar to that of hydrostatic, a 40 K shift (such as that observed for the heavily bombarded sample) would require between 5 and 7 GPa of applied pressure. It is unlikely that the thermal expansion mismatch between $SrRuO_3$ and $SrTiO_3$ in the temperature range of interest would result in such large pressures, or that a $SrRuO_3$ thin film could support such a load without fracture.

D. Proposed mechanism

It is believed that structural disorder caused by energetic bombardment is responsible for at least part of the T_c depression. A similar depression of the transition temperature has been observed in ferroelectric films and was attributed to a subgrain structure which defined a finite size of coherently diffracting material.[31] A second possibility which may explain the reduction in T_c and the differences in resistivity values is a deposition pressure-dependent film composition. Unfortunately, accurate compositional characterization of epitaxial $SrRuO_3$ is difficult due to the inability to dissolve $SrRuO_3$ and the overlap of the peaks associated with Sr and Ru in a Rutherford backscattering spectrum. In any case, judging from other work on nonvolatile perovskite crystals, the composition differences are probably modest and within the confidence limits of standard characterization methods.[22]

The extended lattice constants in $SrRuO_3$ are believed to be a result of energetic bombardment by the ionized and neutral target species accelerated by means of plume expansion. Due to the nature of laser–solid interactions, complicated combinations of positive, negative, and neutral species exist in the plasma. This makes direct quantitative analysis difficult in comparison to sputtering plasmas where species' energy and population may be well known.[19] Many studies of laser-induced plasmas have been reported, and indicate that at sufficiently low pressures and sufficiently small target-to-substrate separation distances, bombarding species with enough energy to damage solids impinge upon the substrate. Zheng *et al.*[32] reported, for the deposition of $YBa_2Cu_3O_{7-\delta}$ in vacuum, mean kinetic energies between 40 and 85 eV for the associated ionic species at a distance of 7 cm from the target surface; time-of-flight mass spectrometry was used. Using optical emission to study a lead zirconate titanate plasma plume, Kurogi *et al.*[33] observed 60 eV titanium species 5 cm from the target under vacuum conditions. Furthermore, as pressures were increased to 200 mTorr, the energy of the titanium species were found to decrease to <1 eV, thus indicating that as ambient pressures in PLD are increased, sufficient thermalization occurs, resulting in plasma species in the vicinity of the substrate with near kT energies. These studies clearly indicate that laser–solid inter-

actions in vacuum produce species with energies large enough to damage the solid surfaces upon which they impinge. Sigmund[34] studied the effects of the Si^+ bombardment of Si surfaces both theoretically and experimentally. His findings indicated that the energy threshold for vacancy production by atomic displacement was ~ 16 eV: energies easily achieved by laser plasma species. The penetration depth of the ions as determined by TRIM-code calculation was ~ 5 Å. In PLD, since the bombardment is occurring *in situ* with film growth, 5 Å penetration would be sufficient to produce a defective or damaged crystal through the entire thickness.

It is clear that the extension of lattice constants is coupled with energetic bombardment during deposition, however, the mechanism responsible for the lattice constant extension is not well understood. Possibilities include collision-induced displacement of cations into nonequilibrium lattice locations, implantation of Sr, O, or Ru, resputtering of Sr or Ru, or composition differences resulting from relative cation distributions in the laser plasma which are pressure dependent.[18] Marwick *et al.*[25] observed a similar effect in the electrical properties of $YBa_2Cu_3O_{7-\delta}$ after O^+ ion bombardment; with increased amounts of exposure, a metal-insulator transition was induced. Such a transition in our samples was not observed. However, the data suggest that with sufficiently reduced pressure a sign reversal in the temperature coefficient of the resistivity at low temperatures might occur. Such an observation has been reported by Hiratani *et al.*[24] at deposition pressures below 10 mTorr, although they attributed their effect to the oxidation state of the constituent cations.

The final observation which needs to be addressed is the substrate influence on the lattice constant extension. Under identical deposition conditions, $SrRuO_3$ films deposited on $SrTiO_3$ substrates will exhibit more extended in- and out-of-plane lattice constants than those deposited on $LaAlO_3$. Assuming that the substrate has a negligible affect on the film composition, the only apparent difference between films deposited on $SrTiO_3$ and $LaAlO_3$, with the exception of lattice constant extension, is the mosaic structure as determined by x-ray diffraction line broadening. For films deposited on $LaAlO_3$, the FWHM peak breadth in all circles is at least double that measured for films on $SrTiO_3$. Knowing this, it is suggested that the lattice constant extension is influenced by the crystalline perfection of the growing film. In particular, a channeling effect which enhances the bombardment is proposed. Channeling is well documented to occur during the ion implantation of Si crystals even for large implanted species, e.g., Ge^+ and As^+. Such channeling during implantation is often difficult to avoid.[35] The higher quality $SrRuO_3$ crystals grown on $SrTiO_3$ have a narrower mosaic spread, which may provide more efficient pathways through which the shallowly implanted ablatant can travel. In contrast, the more pronounced subgrain structure of the films deposited on $LaAlO_3$ may reduce their penetration depth and the associated effects which lead to extended lattice constants. He^{2+} channeling yields for $SrRuO_3$ on $SrTiO_3$ and $LaAlO_3$ have been reported as 1.8% and 2.5%, respectively; thus demonstrating the improved ability of ions to channel through structurally refined $SrRuO_3$.[2,3]

IV. CONCLUSIONS

Both the lattice constants and electrical properties of $SrRuO_3$ epitaxial thin films were found to depend upon the deposition pressure during growth by PLD. In general, as the deposition pressure was reduced, the in- and out-of-plane unit cell parameters became extended. In addition to this structural anomaly, the electrical resistivity was found to increase and the Curie temperature shifted to lower values. Though the $SrTiO_3$ substrates were only miscut $-0.5°$, at higher pressure conditions (160 mTorr), $SrRuO_3$ films grew as single crystals. STM images reveal that the films grow by step flow on $SrTiO_3$. Moreover, the films exhibited a smoother topography with less step bunching when deposited at higher pressures. Experiments involving a mixed O_2/O_3:Ar atmosphere illustrated that the extended lattice constant effect was due to energetic bombardment of the film surface during growth. $SrRuO_3$ films were also deposited onto $LaAlO_3$ substrates. The deposition pressure necessary to produce bulk lattice constants on $LaAlO_3$ was at least a factor of 2 smaller than that required when using $SrTiO_3$ substrates, i.e., these samples could withstand more aggressive deposition conditions. It is proposed that more efficient channeling of the plume species into the highly crystalline $SrRuO_3$ films is responsible.

[1] R. J. Bouchard and J. L. Gillson, Mater. Res. Bull. **7**, 873 (1972).
[2] X. D. Wu, S. R. Foltyn, R. C. Dye, Y. Coulter, and R. E. Muenchausen, Appl. Phys. Lett. **62**, 2434 (1993).
[3] C. B. Eom, R. J. Cava, R. M. Flemming, J. M. Phillips, R. V. van Dover, J. H. Marshall, J. W. P. Hsu, J. J. Krajewski, and J. W. F. Peck, Science **258**, 1766 (1992).
[4] C. W. Jones, P. D. Battle, P. Lightfoot, and W. T. A. Harrison, Acta Crystallogr., Sect. C: Cryst. Struct. Commun. **45**, 365 (1989).
[5] L. Mieville, T. H. Geballe, L. Antaonazza, and K. Char, Appl. Phys. Lett. **70**, 126 (1997).
[6] G. Cao, S. McCall, and J. E. Crow, Phys. Rev. B **55**, R672 (1997).
[7] A. Callaghan, C. W. Moeller, and R. Ward, J. Inor. Chem. **5**, 1572 (1966).
[8] Micro is a trademark of International Products Corporation, Burlington, NJ.
[9] M. Kawasaki, K. Takahashi, T. Maeda, R. Tsuchia, M. Shinohara, O. Ishiyama, M. Yoshimoto, and H. Koinuma, Science **266**, 1540 (1994).
[10] PCI Ozone Corporation, West Caldwell, NJ.
[11] Baratron is a trademark of MKS Instruments, Andover, MA.
[12] Target Materials International, Columbus, OH.
[13] B. D. Cullity, *Elements of X-ray Diffraction* (Addison-Wesley, Reading, 1978).
[14] D. T. Rooney, J. B. Dixon, K. G. Schurr, and M. R. Northrup, Int. J. Micro. Elec. Pack. **20**, (1997).
[15] Alphastep 2000, Tencor Instruments, Mountain View, CA.
[16] *Pulsed Laser Deposition of Thin Films*, edited by D. B. Chrisey and G. K. Hubler (Wiley, NY, 1994).
[17] B. Holzapfel, B. Roas, L. Schultz, P. Bauer, and G. Saemann-Ischenko, Appl. Phys. Lett. **61**, 3178 (1992).
[18] A. Jukna, B. Vengalis, F. Anisimovas, and V. Jasutis, Vacuum Proceedings of the 4th European Vacuum Conference, Volume 46, Numbers 8–10 (1995), pp. 977,978.
[19] D. Smith, *Thin-Film Deposition* (McGraw-Hill, New York, 1995).
[20] Q. Gan, R. A. Rao, and C. B. Eom, Appl. Phys. Lett. **70**, 1962 (1997).
[21] E. J. Tarsa, E. A. Hachfeld, F. T. Quinlan, and J. S. Speck, Appl. Phys. Lett. **68**, 490 (1996).
[22] J.-P. Maria, M.S. thesis, The Pennsylvania State University, 1996 (unpublished).

[23] J. K. Burdette, *Chemical Bonding in Solids* (Oxford University Press, New York, 1995).
[24] M. Hiratani, C. Okazaki, K. Imagawa, and K. Takagi, Jpn. J. Appl. Phys., Part 1 **33**, 6212 (1996).
[25] A. D. Marwick, G. J. Clark, K. N. Tu, D. S. Lee, U. N. Singh, J. Doyle, and J. J. Cuomo, Nucl. Instrum. Methods Phys. Res. B **40/41**, 612 (1989).
[26] L. Klein, J. S. Dodge, T. H. Geballe, A. Kapitulnik, A. F. Marshall, L. Antognazza, and K. Char, Appl. Phys. Lett. **66**, 2427 (1995).
[27] L. Klein, J. S. Dodge, C. H. Ahn, G. D. Snyder, T. H. Geballe, M. R. Beasley, and A. Kapitulnik, Phys. Rev. Lett. **77**, 2774 (1996).
[28] M. Shepard, G. Cao, S. McCall, F. Freibert, and J. E. Crow, J. Appl. Phys. **79**, 4821 (1996).
[29] M. Shikano, T. Huang, M. Itoh, and T. Nakamura, Solid State Commun. **90**, 115 (1994).
[30] J. J. Neumeier, A. L. Cornelius, and J. S. Schilling, Physica B **198**, 324 (1993).
[31] J.-P. Maria, S. Trolier-McKinstry, and D. G. Schlom, Proceedings of the 10th IEEE International Symposium on Applied Ferro. 1, 1996, pp. 333–337.
[32] J. P. Zheng, Z. Q. Huang, D. T. Shaw, and H. S. Kwok, Appl. Phys. Lett. **54**, 280 (1989).
[33] H. Kurogi, Y. Yamagata, T. Ikegami, K. Ebihara, B. Y. Tong, and K. Kumamoto, Mater. Res. Soc. Symp. Proc. **433**, 237 (1996).
[34] P. Sigmund, Appl. Phys. Lett. **14**, 114 (1969).
[35] S. Wolf and R. N. Tauber, *Silicon Processing for the VLSI Era*: Vol. 1 (Lattice, Sunset Beach, 1986).